© 2016. Published by The Company of Biologists Ltd | Development (2016) 143, 1302-1312 doi:10.1242/dev.126714

An *in vitro* model of hemogenic endothelium commitment and hematopoietic production

Laurent Yvernogeau[1,2,*], Rodolphe Gautier[1,2], Hanane Khoury[1,2], Sara Menegatti[1,2,‡], Melanie Schmidt[1,2], Jean-Francois Gilles[3] and Thierry Jaffredo[1,2,§]

ABSTRACT

Adult-type hematopoietic stem and progenitor cells are formed during ontogeny from a specialized subset of endothelium, termed the hemogenic endothelium, via an endothelial-to-hematopoietic transition (EHT) that occurs in the embryonic aorta and the associated arteries. Despite efforts to generate models, little is known about the mechanisms that drive endothelial cells to the hemogenic fate and about the subsequent molecular control of the EHT. Here, we have designed a stromal line-free controlled culture system utilizing the embryonic pre-somitic mesoderm to obtain large numbers of endothelial cells that subsequently commit into hemogenic endothelium before undergoing EHT. Monitoring the culture for up to 12 days using key molecular markers reveals stepwise commitment into the blood-forming system that is reminiscent of the cellular and molecular changes occurring during hematopoietic development at the level of the aorta. Long-term single-cell imaging allows tracking of the EHT of newly formed blood cells from the layer of hemogenic endothelial cells. By modifying the culture conditions, it is also possible to modulate the endothelial cell commitment or the EHT or to produce smooth muscle cells at the expense of endothelial cells, demonstrating the versatility of the cell culture system. This method will improve our understanding of the precise cellular changes associated with hemogenic endothelium commitment and EHT and, by unfolding these earliest steps of the hematopoietic program, will pave the way for future *ex vivo* production of blood cells.

KEY WORDS: Hemogenic endothelium, Hematopoiesis, Endothelium, Aorta, Avian, Quail

INTRODUCTION

The first hematopoietic stem/progenitor cells (HSPCs) emerge during the initial phase of embryonic development in the form of cell aggregates, designated hematopoietic clusters, that are intimately associated with endothelial cells (ECs) in the floor of the dorsal aorta and in the umbilical and vitelline arteries (Dzierzak and Speck, 2008; Medvinsky et al., 2011). These hematopoietic clusters were shown to be pivotal in the formation of the adult blood system by providing the first adult-type hematopoietic stem cells. Aorta-associated hematopoietic cluster formation has been documented in a variety of vertebrate embryos and thoroughly characterized by immunohistological studies on sections (Jaffredo et al., 2005b) and, more recently, through high-resolution 3D visualization techniques (Yokomizo and Dzierzak, 2010). Tracing experiments *in vivo*, including live imaging approaches, revealed a developmental relationship between ECs and hematopoietic clusters (Jaffredo et al., 1998; de Bruijn et al., 2002; Zovein et al., 2008; Chen et al., 2009; Bertrand et al., 2010; Boisset et al., 2010; Kissa and Herbomel, 2010; Lam et al., 2010). Cluster emergence relies on the presence of specialized ECs, termed hemogenic endothelial cells, which, upon appropriate signaling (Richard et al., 2013), lose their endothelial phenotype and acquire hematopoietic traits. This complex, multi-step developmental process was designated the endothelial-to-hematopoietic transition (EHT) (Kissa and Herbomel, 2010). During EHT, hematopoiesis was shown to occur *de novo* at the expense of the hemogenic endothelium compartment that is progressively lost (Pouget et al., 2006; Kissa and Herbomel, 2010).

Since the hemogenic endothelium represents a small fraction of the ECs and is found only during the early stages of development in the aorta and the associated arteries, a number of efforts have been devoted to design *in vitro* models that faithfully recapitulate hemogenic endothelium commitment and hematopoietic production. The most robust and reliable system was obtained with the use of embryonic stem cells (ESCs). Using appropriate culture conditions, ESCs undergo differentiation and form cellular structures containing progenitors, termed blast colony-forming cells, that are able to give rise to colonies comprising both blood cells and ECs (Choi et al., 1998). Comparing *in vitro* cultures with the *in vivo* situation in the early mouse embryo, the blast colony-forming cell was shown to be the *in vitro* equivalent of the nascent mesoderm ingressing through the primitive streak (Huber et al., 2004) and was characterized by the expression of the receptor tyrosine kinase Flk1 (also known as Kdr and Vegfr2) and the T-box transcription factor brachyury (Robertson et al., 2000). Using well-established culture systems, it was possible to drive this early mesodermal progenitor to differentiate into hemogenic ECs able to give rise to blood cells through EHT and to document several aspects of blood formation from hemogenic ECs (Eilken et al., 2009; Lancrin et al., 2009), including some aspects of EHT (Ditadi et al., 2015). However, the number of hemogenic ECs generated in ESC cultures was reported to be low (1/3000) (Eilken et al., 2009), hampering the establishment of a versatile culture system that could be employed to address questions concerning hemogenic endothelium commitment from non-hemogenic ECs and the cellular and molecular changes that occur during EHT.

The pre-somitic mesoderm (PSM), or paraxial mesoderm, gives rise to the somites and contains numerous progenitor cells able to differentiate into the various lineages produced by the somites. In

[1]Sorbonne Universités, UPMC Univ Paris 06, IBPS, UMR 7622, Laboratoire de Biologie du Développement, Paris 75005, France. [2]CNRS, UMR 7622, Inserm U 1156, IBPS, Laboratoire de Biologie du Développement, Paris 75005, France. [3]Institute of Biology Paris-Seine, Sorbonne Universités, UPMC Univ Paris 06, Cellular Imaging Facility, Paris 75005, France.
*Present address: Hubrecht Institute, Uppsalalaan 8, Utrecht 3584 CT, The Netherlands. ‡Present address: Cancer Research UK Manchester Institute, The University of Manchester, Wilmslow Road, Manchester M20 4BX, UK.

§Author for correspondence (thierry.jaffredo@upmc.fr)

Received 22 May 2015; Accepted 21 February 2016

Development (2016) 143, 1302-1312 doi:10.1242/dev.126714

addition to the axial skeleton, skeletal muscles and dermis, the PSM has also been shown to produce a small cohort of ECs that give rise to vascularization of the body wall and limbs and contribute to the aortic roof (Pardanaud et al., 1996; Pouget et al., 2006; Yvernogeau et al., 2012). Of note, somite-derived ECs, which are not initially endowed with hemogenic potential, can be turned into hemogenic cells following exposure to endoderm or to growth factors mimicking the endoderm (Pardanaud and Dieterlen-Lièvre, 1999). Hence, the PSM appears to be a source of naïve mesodermal progenitors that can be orientated towards various cell types upon exposure to the appropriate signals. Given the accessibility of PSM, we reasoned that it could be used as an *in vitro* model in which to trigger the differentiation of large numbers of ECs and hemogenic ECs able to recapitulate the cellular events occurring in the aorta at the time of hematopoietic production.

Here, we report the development of such an *in vitro*, feeder-free culture system that allows the commitment of naïve mesodermal cells *en masse* into hemogenic ECs that are able to undergo robust and long-lasting hematopoiesis over a period of at least 2 weeks. The approach uses pieces of PSM that are submitted to a cocktail of growth factors that drives them to differentiate into ECs. Hemogenic ECs, characterized by the expression of the transcription factor RUNX1, are specified from cells already expressing endothelial markers. Single-cell tracking of hemogenic ECs allows capture of the ephemeral flat-to-round cell transition and revealed unexpected traits of EHT. Moreover, by modulating the combination of growth factors it is possible to preclude EC commitment, accelerate EHT or to promote smooth muscle cell versus EC differentiation. The design of this robust, highly reproducible *in vitro* model will improve our understanding of the precise cellular and molecular changes associated with EHT and will pave the way for the future *ex vivo* production of blood cells and potentiate the discovery of blood cell modulators.

RESULTS

PSM as a naïve mesodermal tissue

Somites are segmental mesoderm derivatives known to be pivotal in the formation of vertebrate embryos by producing a variety of cell types, including skeletal muscles, dermis of the back, tendon, axial skeleton and endothelium of the body wall and limbs (Christ et al., 2007). The somites differentiate from the rostral end of the PSM, a band of loose mesenchyme that does not exhibit any segmental pattern but expresses an ensemble of oscillatory genes to form the somites (Pourquie, 2003). Taking advantage of previous experience with the *in vivo* manipulation of pieces of mesoderm from early embryos (Pardanaud and Dieterlen-Lièvre, 1999), we hypothesized that this tissue could serve as a source for naïve mesoderm that could be orientated towards the endothelial lineage and, more specifically, towards the hemogenic endothelial lineage following exposure to the appropriate signals.

Quail PSM was isolated as described (Pouget et al., 2006; Yvernogeau et al., 2012), free of surrounding contaminating tissues (Fig. 1A, Movie 1). We chose this species because our previous work was based on the use of quail PSM (Pouget et al., 2006) and because

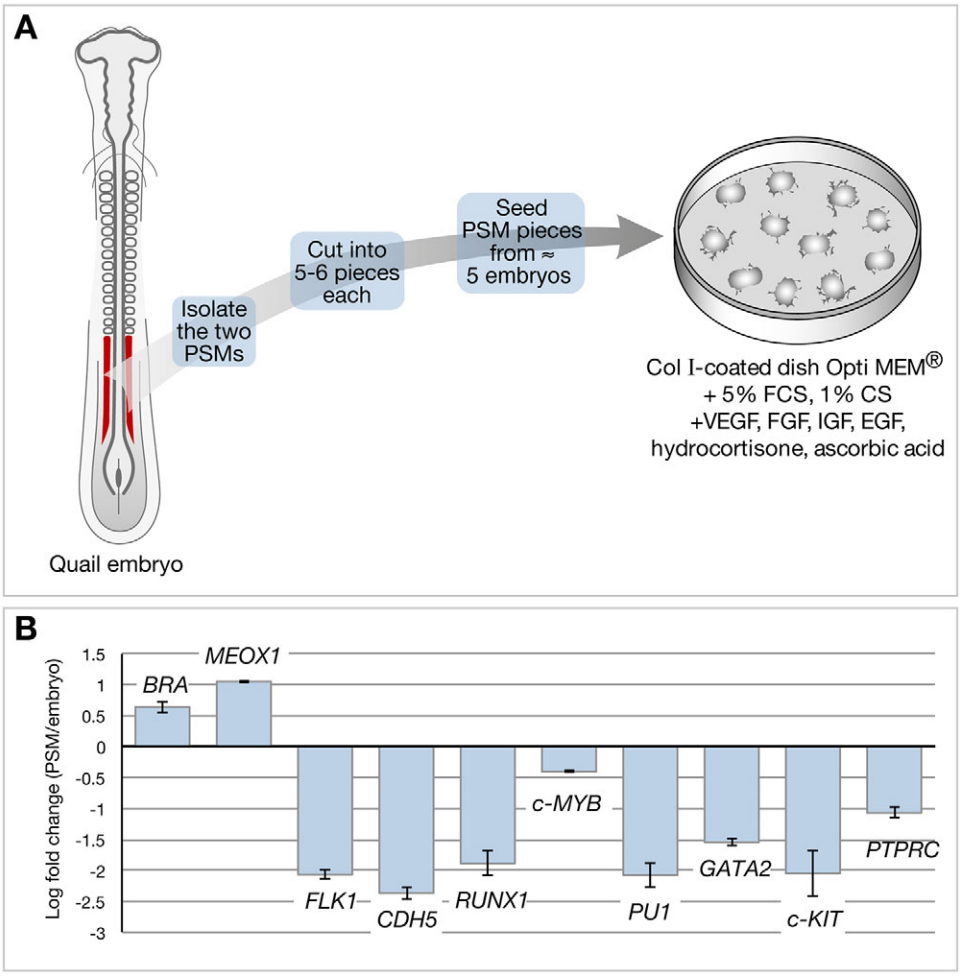

Fig. 1. Culture system and molecular identification of the PSM. (A) The two quail PSMs (red) encompassing a length of about ten somites were isolated, cut into five or six pieces each, and placed in 35-mm culture dishes coated with collagen I. Ten PSMs were plated per dish in Opti-MEM in the presence of 5% fetal calf serum, 1% chicken serum, VEGF, FGF, IGF, EGF, hydrocortisone and ascorbic acid. Cultures were followed over a period of 12 days and time-lapse imaged at different time points. (B) qRT-PCR analysis showing the identity of the PSM through the expression of mesodermal, endothelial and hematopoiesis-specific genes. A positive/negative fold change represents upregulation/downregulation, respectively, of expression in the PSM relative to the same stage embryo. RNA for qPCR was obtained by pooling ten PSMs from five embryos of the same stage. *n*=2 independent experiments. Error bars indicate s.d.

Development (2016) 143, 1302-1312 doi:10.1242/dev.126714

quail cells are known to display greater multiplication potential in culture than chicken cells. PSM was submitted to qRT-PCR analysis to probe the expression of mesoderm genes as well as endothelial and hematopoiesis-specific genes (Fig. 1B). Indeed, the PSM expressed brachyury (*BRA*), which encodes a T-box molecule that is expressed by epiblast cells and by the nascent mesoderm following gastrulation (Wilkinson et al., 1990; Kispert et al., 1995), and *MEOX1*, which is specific for uncommitted mesoderm and trunk paraxial mesoderm, but was free of endothelial and hematopoiesis-specific gene expression indicating that none of these lineage commitments has occurred at the time of PSM isolation.

Design of culture conditions and the observation of cultures

We tested different culture media and extracellular matrices that could favor adhesion and the differentiation of PSM-derived cells towards the endothelial lineage. The pieces of PSM exhibited a poor capacity to spread in the absence of extracellular matrix (not shown). Since collagen was reported to positively regulate EC commitment and migration (Whelan and Senger, 2003; Lamalice et al., 2007), we compared collagen I and IV in their efficacy to support endothelial differentiation. Based on cell morphology (Hirashima et al., 2003; Guo et al., 2007; Eilken et al., 2009), type I collagen-coated dishes offered a better differentiation of PSM cells than type IV collagen-coated dishes (not shown). We initially used a cocktail of growth factors from Lonza (SingleQuots Kit) reported to improve the growth of primary EC cultures. However, owing to lack of information regarding the concentrations of the individual growth factors, we decided to replace this cocktail by one of the same composition but using individually purchased growth factors of known concentration. Having chosen the medium (Opti-MEM) and the support (35-mm collagen I-coated dish), the following human growth factors and supplements known to work on avian cells (our unpublished work) were added to Opti-MEM/fetal calf serum (5%)/chicken serum (1%)/penicillin-streptomycin (100 units/ml): VEGF (2 ng/ml), FGF (4 ng/ml), IGF (3 ng/ml), EGF (10 ng/ml), hydrocortisone (200 ng/ml) and ascorbic acid (75 ng/ml).

The culture conditions being defined, we then followed morphological aspects of the culture over a period of 12 days (D). Retrospectively, the culture period could be divided into three phases: (1) spreading and EC differentiation from D0 to D3-4; (2) hematopoietic cell (HC) emergence and production from D4-5 to D8-9; (3) the continuation of HC production and multiplication from D8-9 to D12. During the first 24-48 h of culture (D0 to D2), the pieces of PSM spread onto the collagen I-coated dishes, forming flat layers of tightly adherent cells that displayed EC-like morphology (Fig. 2A-C, Movie 2). From D4, isolated cells among the layer of ECs began to produce round cells that detached from the culture (Fig. 2D). Their number increased over the next few days to form large areas covering the EC layer beneath (Fig. 2E,F). From this period, their number increased further to invade the whole culture dish within the next 3-4 days (Fig. 2G). Flow cytometry analysis using a monoclonal antibody recognizing the QH1 antigen (hereafter referred as to QH1), as a marker for endothelial and hematopoietic cells (Pardanaud et al., 1987) indicated that, at D4, ~70% of the cells were $QH1^+$ (Fig. 2H), as confirmed by QH1 immunocytological staining of the culture (Fig. 2I,J). The EC phenotype was also confirmed using the uptake of human AcLDL as readout (Fig. 2K,L).

Molecular characterization of the culture

We monitored the culture over a period of 12 days and analyzed the expression of gene sets representative of naïve mesoderm, endothelium, hemogenic endothelium and hematopoietic cells using semi-quantitative RT-PCR (Fig. 3A), with validation of some key genes using qPCR (Fig. 3B-D). From D0 to D6, cultures were analyzed daily, and every 2 days from D6 to D12.

BRA was detected immediately following culture onset and during D1, but was no longer expressed at D2. Initially absent at the onset of culture, *FLK1* expression appeared at D0.5-D1. Co-expression of *BRA* and *FLK1*, reported to be associated with the hemangioblast stage (Huber et al., 2004; Vogeli et al., 2006), was detected between D0.5 and D1. The transcription factor *SCL* (also known as *TAL1*), which is crucial for the emergence of the hematopoietic and endothelial lineages during embryoid body differentiation (Lancrin et al., 2009), was found to be expressed from D0.5, as was *GATA2*, which is known to be expressed by mesoderm and nascent ECs (Elefanty et al., 1997; De Val and Black, 2009). Expression of the genes encoding the endothelial and hematopoietic progenitor cell antigen CD34 (Tavian et al., 1996; Wood et al., 1997) and, to a weaker extent, the endothelial-specific calcium-dependent cell adhesion molecule CD144 (also known as cadherin 5) (see also Fig. 3B), was activated at the same time, indicating that endothelial commitment has occurred. This was accompanied by the onset of expression of *CD31* (also known as *PECAM1*), which is expressed on endothelial and hematopoietic cells during development (Newman et al., 1990), and of *vWF*, a key marker of EC function (Wagner et al., 1982), supporting a dynamic EC commitment. Of note, *RUNX1*, a key gene in the generation of blood from the hemogenic endothelium, was expressed at low levels from D0.5 and was significantly upregulated from D3, suggesting that hemogenic endothelium differentiation occurred shortly after the onset of culture. Taken together, ECs differentiated from D0.5, shortly followed by hemogenic ECs.

The culture persisted free of hematopoietic cells until D3. From D3 onwards, the myeloid- and B lymphoid-specific transcriptional activator *PU1* (also known as *PU.1* or *SPI1*) was expressed, shortly followed by *CD45* (also known as *PTPRC*), a pan-hematopoietic marker during development, indicating that hematopoietic commitment had occurred (see also Fig. 3C,D for a more quantitative analysis). *PU1* and *CD45* expression were significantly reinforced from D5, which is when the production of round cells first became prominent. From D6, most of the markers maintained their expression until the end of the culture period at D12.

In order to confirm the commitment into hemogenic endothelium, cultures were co-stained for AcLDL and with an antibody against RUNX1 from D0 to D3. RUNX1 expression was detectable by immunocytochemistry by D2. At this time, only a few $AcLDL^+$ cells expressed RUNX1. The number of $RUNX1^+$ cells dramatically increased at D3 (Fig. 3E-G, Fig. S1A-C), 1 day before the first conspicuous EHT events.

Characterization of the non-adherent cells

We characterized the non-adherent cell fraction from D4, the onset of their production, to the end of the culture period at D12, when non-adherent cells were present in large numbers. Non-adherent cells are hereafter designated as the floating (F) fraction followed by a number indicating their day of retrieval from the culture, i.e. F6 refers to non-adherent cells collected on D6. Non-adherent cells were collected daily from D4 to D12 by thoroughly rinsing the culture dishes, and were counted. A mean of $2\text{-}3\times10^4$ cells were produced daily from F4 to F10. By F10, the production increased to reach 1.04×10^5 cells by F12 (Fig. 4A). This increase is at least partly due to the multiplication of the non-adherent cells, as documented in Movie 3.

Development (2016) 143, 1302-1312 doi:10.1242/dev.126714

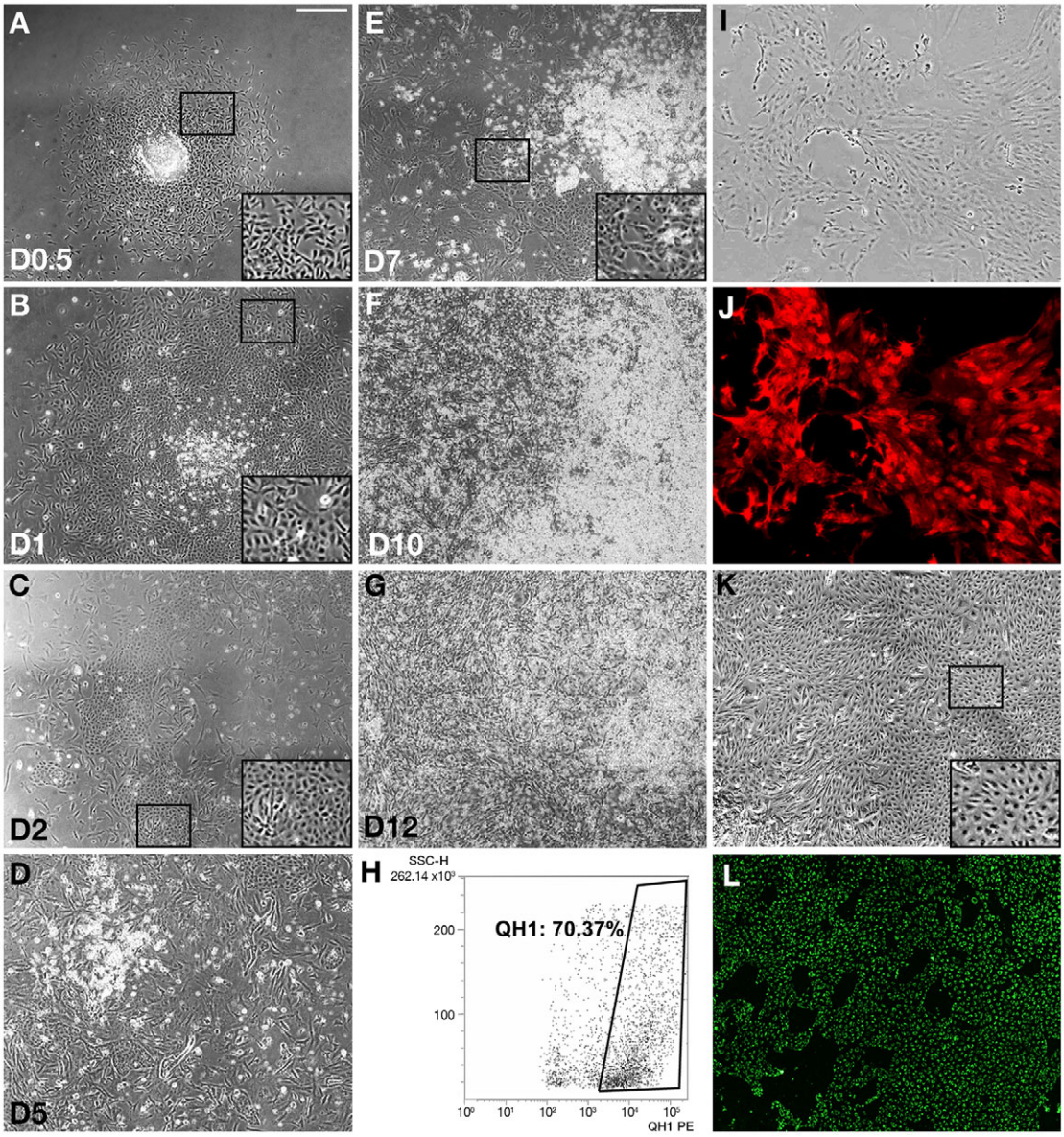

Fig. 2. Morphology and characterization of the culture over time. (A-G) Observation of the culture over a period of 12 days. (A) D0.5, showing initial spreading of a PSM piece. (B) D1, showing the spread of cells to form a flat layer of tightly attached cells, except for the center where spreading is still in progress. (C) D2, showing that cells unable to spread in the center have died. Large areas of adherent cells displaying EC sheet morphology are clearly visible. (D) D5, the beginning of the budding process. Some round, hematopoietic-like floating cells are visible either as single cells or as aggregates of refracting cells. (E) D7, when large aggregates of refracting cells are visible, with the flat layer of cells displaying EC sheet morphology beneath. (F) D10, the number of round, hematopoietic-like cells has significantly increased to cover large areas of the culture dish. (G) D12, the culture is now covered with round cells. The presence of flat EC-like cells has significantly decreased. Scale bar: 100 µm. (H) Flow cytometry analysis of the culture at D4 with the monoclonal antibody QH1. About 70% of the cells, which are mostly flat, attached cells at that stage, are $QH1^+$, testifying to the prominent presence of endo-hematopoietic cells. (I,J) Immunofluorescent characterization of the flat cells using the QH1 monoclonal antibody at D4. Flat cells clearly display cell surface QH1 (J, red), indicative of their endothelial phenotype. (I) Phase contrast. (K,L) AcLDL uptake. Living cells were submitted to AcLDL-A488 uptake for 3 h at 37°C. Endocytic vesicles appear green under UV transillumination. Most of the cells displayed AcLDL uptake (L, green), indicative of their endothelial phenotype. (K) Phase contrast. Insets show higher magnifications of boxed regions.

Since QH1 marks quail endothelial and hematopoietic cells (Pardanaud et al., 1987), we FACS analyzed the floating fraction for QH1 at D7. More than 98% of the cells were $QH1^+$, indicating that they probably exhibit a hematopoietic phenotype (Fig. 4B). FACs analysis results were confirmed by QH1 immunostaining of the non-adherent fraction (Fig. 4C,D).

With the aim of further characterizing these cells, we performed qRT-PCR on the non-adherent fraction from D4 to D12 using key markers of endothelial-to-hematopoietic cell commitment. As expected, *BRA* expression was never detected in floating cells (not shown). *CD144*, a key marker of ECs, was downregulated (Fig. 4E) in keeping with the endothelial-to-hematopoietic commitment analyzed *in vivo*. By contrast, *PU1* (Fig. 4F) and *CD45* (Fig. 4G) were upregulated with time, indicating that a progressive hematopoietic commitment was occurring. Interestingly, *PU1* expression preceded that of *CD45* in accordance with a progressive hematopoietic maturation in culture.

Development (2016) 143, 1302-1312 doi:10.1242/dev.126714

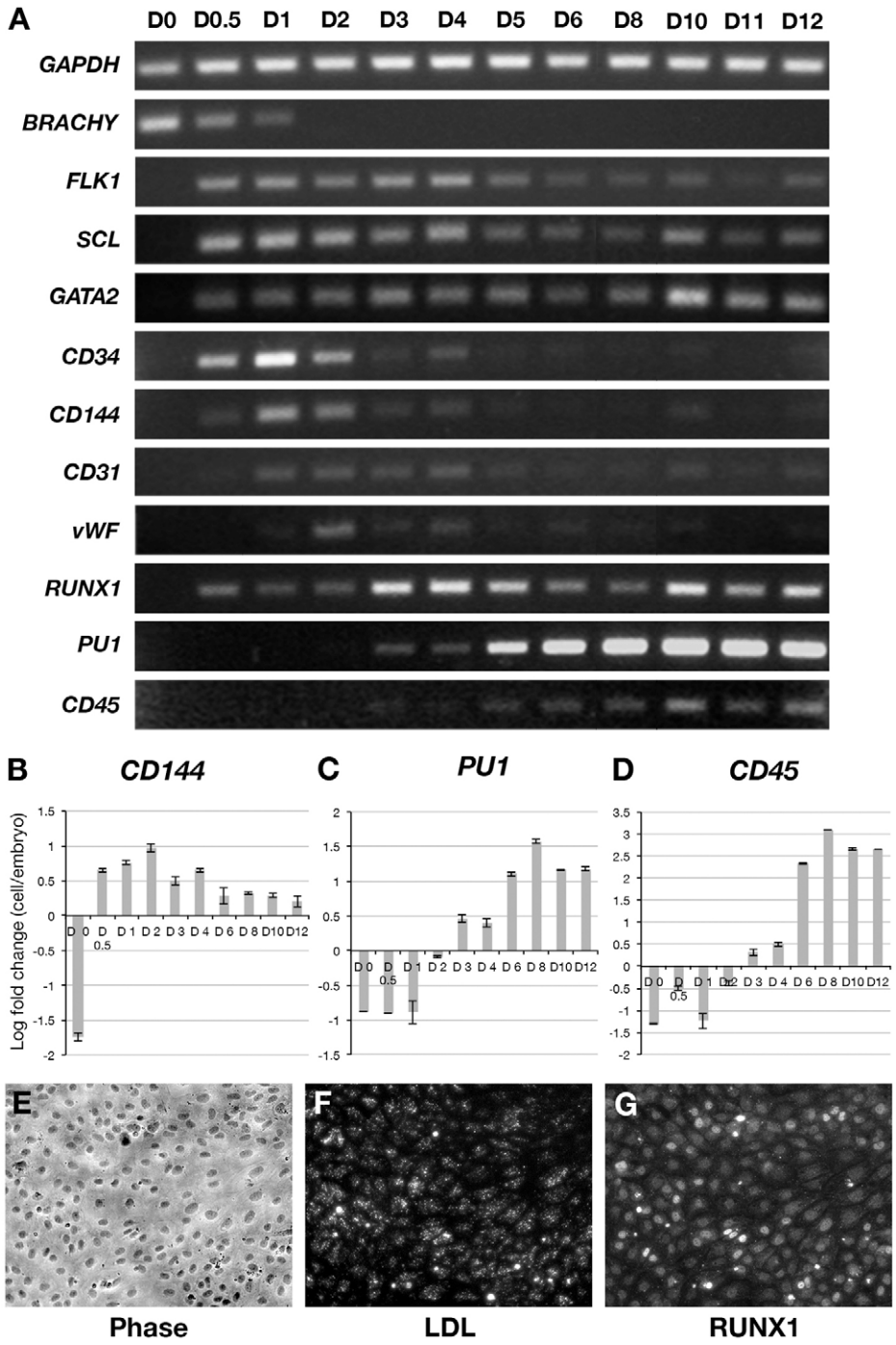

Fig. 3. Molecular characterization of the culture. (A) Semi-quantitative RT-PCR revealing the sequential expression of sets of genes required for mesoderm induction and endothelial and hematopoietic commitment. PCR reactions were run side by side on a 1% agarose gel. Cells from two or three culture dishes were harvested daily from D0 to D6 and every 2 days from D6 to D12. *GAPDH* serves as a control for mRNA amount. A progression from mesoderm to hematopoietic commitment is clearly visible through the expression patterns of several lineage-specific genes (see Results for details). (B-D) qPCR analysis of endothelial, hematopoietic commitment and hematopoietic differentiation-specific genes. The results are shown as the log-transformed fold change in expression (PSM compared with same stage embryo). (B) *CD144*, a recognized endothelial-specific gene, displays a transient increase in expression from D0.5 to D4, then drops and remains low but stable from D6 to D12. (C) *PU1*, one of the earliest genes expressed during hematopoietic commitment, becomes expressed by D3, indicating the onset of EHT. Its expression increased with time and remained high at D12. (D) *CD45*, a hematopoiesis-specific gene, becomes expressed at low level by D3, then is strongly increased by D6 indicative of substantial hematopoietic differentiation and remains high until D12. Error bars indicate s.d. (E-G) Uptake of AcLDL and expression of the transcription factor RUNX1 in D4 cultures. (E) Phase contrast. The flat endothelial-specific phenotype is clearly visible. (F) Cells display prominent uptake of AcLDL. (G) Several cells display high RUNX1 immunostaining in the nucleus, while weaker staining is also visible in most of the cells indicative of their hemogenic endothelial commitment.

To further identify the non-adherent fraction, we collected F6 cells and performed cytospin followed by May–Grünwald Giemsa staining. Thorough characterization of the cells revealed their hematopoietic phenotype and the presence of cells from the granulocyte, erythroblast and monocyte lineages (Fig. 4H).

Tracking EHT

Based on previous characterization, the production of round cells from flat cells faithfully corresponds to an EHT (Jaffredo et al., 1998; Kissa and Herbomel, 2010). Given the high number of hemogenic ECs generated in the culture and the large number of HCs produced, we decided to track EHT using live imaging. Cultures were imaged every 10-15 min over periods from 14-18 h during D3 to D4, when the first EHT events are initiated. To better track EHT, we developed a script running under ImageJ that allows: (1) the labeling of a cell undergoing EHT and to retrospectively identify the flat cell giving rise to the round cell; and (2) to follow the bright, newly formed round cell, over time (see Materials and Methods).

EHT was rapid and left a cell-free area indicating that the fate change occurred at the single-cell level. The passage from flat, adherent cell, to non-adherent cell took between 15 and 30 min. In general, no cell division was detected prior to the passage from flat to round, ruling out asymmetric cell division as a prerequisite for EHT. Round cell production thus caused a progressive exhaustion of the layer of flat cells. Upon detachment, the cell underwent dynamic movements, emitting cellular processes during a period of 30-45 min.

Development (2016) 143, 1302-1312 doi:10.1242/dev.126714

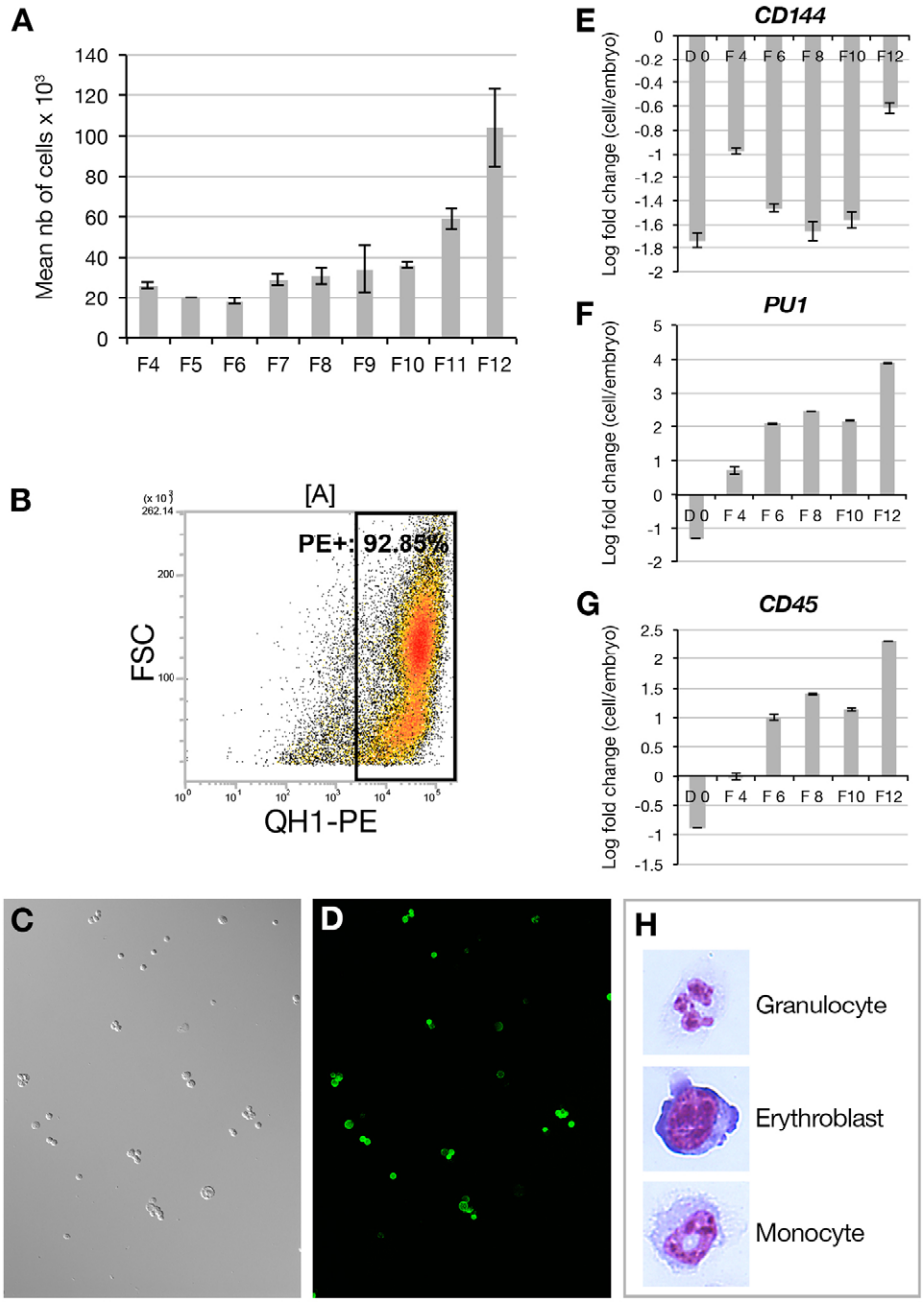

Fig. 4. Characterization of the non-adherent cells. (A) The number of non-adherent cells produced *de novo* in a 35 mm culture dish was followed daily from D4, the onset of production of floating cells, until the completion of the culture at D12. The number of floating cells produced remained at ~2×10^4 daily from D4 to D8 and progressively increased to reach a mean of 1×10^5 at D12. (B) Flow cytometry analysis at D6 indicated that more than 90% of the floating cells displayed strong QH1 immunostaining, indicative of their endo-hematopoietic phenotype. (C,D) Immunohistological characterization of the non-adherent cells by QH1-Alexa 488 staining (D) confirmed the flow cytometry analysis. (C) Phase contrast. (E-G) qPCR analysis of endothelial, hematopoietic commitment and hematopoietic differentiation-specific genes. The results are shown as the log-transformed fold change in expression (PSM versus same stage embryo). (E) *CD144* is strongly downregulated in all the floating fractions tested, indicative of the loss of endothelial-specific gene expression during hematopoietic commitment and differentiation. (F) *PU1* is upregulated from F4, the earliest time point of EHT, followed by an increase in expression with time. (G) *CD45* is upregulated from F6 and increases with time. (H) The non-adherent cells were collected by cytospin and submitted to May–Grünwald Giemsa staining. Erythroblasts and differentiated granulocytes and monocytes were found to be abundant, indicative of multilineage differentiation. Error bars indicate s.d.

Following these movements, cells became round and left the site of production. In rare instances, round cells immediately initiated cell division, whereas the vast majority of round cells that were produced underwent cell division some hours after EHT (Movies 4-6).

Influence of the tissue of origin and the composition of the medium

Given the results obtained with the PSM, we examined whether other conditions could give similar or superior EC commitment. We first compared the PSM with the four last-formed somites and with the lateral plate mesoderm isolated from embryos at the same stage. The pieces of tissue were cultured in the above-described conditions over a period of 4 days, i.e. to just before the initiation of EHT. EC commitment was first assessed based on morphological criteria when ECs were conspicuously visible, and second using FACS analysis following AcLDL uptake. As expected, the PSM gave rise to flat layers of tightly adherent cells that displayed EC-like morphology, whereas the somites and the lateral plate mesoderm showed a poor EC-like differentiation. In addition, cells of the lateral plate did not exhibit robust growth in the culture conditions employed (Fig. S2A,C,E) and FACS analysis was therefore not performed. From three independent experiments the PSM gave a mean of 40±13% $AcLDL^+$ cells, whereas the somites gave a mean of 3±3% (Fig. S2B,D), demonstrating the unique capacity of PSM cells to respond to EC commitment under our culture conditions. It should be noted that this percentage is slightly lower than that we reported using QH1 staining. This might be related to subtle differences in the maturation status of the ECs, i.e. the QH1 antibody recognizes the immature ECs (angioblasts) and the more mature ECs whereas AcLDL stains the mature ECs.

Development (2016) 143, 1302-1312 doi:10.1242/dev.126714

We then analyzed the role of serum in triggering EC commitment. Since the cultures were supplemented with 5% FCS and 1% CS, we withdrew one or other serum and examined the effect on the formation of flat cell layers and on AcLDL uptake by flow cytometry. Imaging and FACS analyses were performed at D4. Interestingly, withdrawal of FCS enhanced EC commitment compared with standard conditions, the percentage of AcLDL$^+$ cells reaching 91.5±0.5% compared with a mean of 40±13% for the PSM in standard conditions (Fig. 5A-D,I). By contrast, removal of CS resulted in a slight, non-significant decrease in the cell population taking up AcLDL at D4 (Fig. 5E,F). However, CS absence significantly impaired cell survival after D4, resulting in substantial cell death at D6-D7 (not shown). As a baseline, we also compared somite tissue in the standard conditions (Fig. 5G,H). Taken together, this analysis revealed that the removal of FCS has a dramatic effect on EC differentiation, strongly promoting the EC phenotype.

Since VEGF and FGF are reported to be potent inducers of angiogenesis and to synergize to promote vascular differentiation (Pepper et al., 1992; Asahara et al., 1995; Seghezzi et al., 1998), we focused on these two factors by analyzing their influence on EC commitment from the PSM. We removed one or other factor or both; we also removed all of the growth factors except VEGF. A morphological analysis was performed at D1 and D4 (Fig. S3). The absence of VEGF caused a phenotype very similar to that when FCS is removed, with a robust emergence of flat, tightly adherent cells at D1 and the presence of very large areas of flat cells even at D3 (Fig. S3C,D, compare with Fig. S3A,B). Removal of FGF, or both VEGF and FGF, resulted in poor EC differentiation at D5 with no visible flat cell area (Fig. S3E-H). When VEGF was added as the sole growth factor, EC differentiation occurred but was readily followed by the substantial production of round, hematopoietic cells as soon as D2 (Fig. S3I,J).

Finally, since the PSM generates several different cell types, we questioned whether it is possible to direct the PSM cells towards the smooth muscle cell lineage. TGFβ, which is known to promote smooth muscle cell differentiation in culture, was added at 25 ng/ml to PSM cultures at D0 and replaced the initial set of growth factors. The layer of cells readily displayed a fibroblast-like morphology, with elongated cells forming a compact layer (Fig. 5J,K). No budding cell was found. Expression of *FLK1*, *SCL*, *PU1* and *CD45* was absent from the culture, and *CD31* was barely detected at D2 and decreased thereafter (Fig. 5L), indicating a blockade in EC commitment. Surprisingly, *RUNX1* expression was still detected but was not associated with *PU1* expression, one of its target genes. By contrast, alpha smooth muscle actin (*αSMA*) mRNA was strongly detected (Fig. 5L), suggesting firm commitment towards the smooth muscle cell lineage. These results demonstrated the phenotypic plasticity of the PSM culture according to the culture conditions.

DISCUSSION

Here, using an easily amenable source of mesoderm, we report the establishment and tuning of a versatile culture system using PSM cells that, with appropriate culture conditions, are able to faithfully recapitulate the cellular events that take place during the formation of the aorta and HSPC production. A notable feature is the bias towards the hemogenic endothelium lineage and the subsequent production of hematopoietic cells through EHT; another is the fact that a large number of cells undergo EHT, making it possible to easily track cell fate changes at a single-cell level using time-lapse video microscopy.

The production of HSPCs from ECs was first shown in the chicken embryo in dye-marking studies (Jaffredo et al., 1998). Using interspecies grafting experiments, it was shown that HSPCs are produced at the expense of the hemogenic endothelial population, which progressively disappeared from the aortic floor (Pouget et al., 2006). In mammalian embryos, phenotypic and genetic approaches also demonstrated that the first HSPCs are derived from vascular ECs during a short period of time (de Bruijn et al., 2002; North et al., 2002; Zovein et al., 2008; Chen et al., 2009). Given the key role of the hemogenic endothelium and EHT in the production of HSPCs, an in-depth investigation of the cellular and molecular processes associated with these traits is needed.

A major hurdle in dissecting hemogenic endothelium commitment and EHT is the low number of cells per embryo coupled with the difficulties in isolating discrete steps associated with the cellular progression. Significant advances have been made, using transgenic mouse lines carrying the +23 *Runx1* hematopoietic enhancer (Swiers et al., 2013), in understanding the molecular control of the endothelial-hematopoietic balance and the timing of these changes. However, hemogenic EC isolation remains difficult, especially if one is to dissect discrete steps from non-hemogenic EC to EHT. Our culture system allows 50-70% of the cells to be directed towards the endothelial and the hemogenic endothelial fates. This is an important advance compared with the number of cells exhibiting these or similar phenotypes in ESC cultures (Eilken et al., 2009) or in embryos *in vivo* (Kissa and Herbomel, 2010; Yokomizo and Dzierzak, 2010). In addition, the stromal cell lines sometimes used in ESC differentiation protocols into EC (Guo et al., 2007) or hemogenic EC (Eilken et al., 2009) are not required in our system, which facilitates cell isolation if needed. Another interesting feature is the fact that EHT and hematopoietic commitment occur without any modification to the composition of the medium. This indicates that the culture conditions faithfully recapitulate the molecular events occurring during endothelial and hemogenic endothelial commitment in the embryonic aorta. Indeed, somitic ECs are not hemogenic, but it has been shown that when these cells are placed in appropriate conditions they are able to give rise to hemogenic ECs and to blood (Pardanaud and Dieterlen-Lièvre, 1999). In our case, we strongly bias the PSM cells towards the EC lineage and turn these non-hemogenic ECs into hemogenic ECs, as testified by the acquisition of endothelial traits followed by *RUNX1* expression during the first 4 days of culture.

Our daily molecular analysis indicates a progressive switch from the mesoderm to the hematopoietic state, with a passage through mesoderm, endothelium, hemogenic endothelium and hematopoietic fates. This is consistent with the proposed model of blood cell formation deduced from ESC cultures (Lancrin et al., 2010). We found that the initial commitment of mesodermal cells into EC from D0 to D2 is not associated with *RUNX1* expression. However, *RUNX1* is expressed in culture from D2, and its expression increases and extends to most, if not all, ECs thereafter. This is in keeping with the changes in *RUNX1* expression shown to occur *in vivo* during the formation of the aorta (Richard et al., 2013), thereby demonstrating that our culture conditions accurately reproduce the cellular and molecular events taking place *in vivo*. When they undergo EHT, each culture produces *de novo* at least 2×10^4 cells per 35-mm dish per day from D4 to D8, and this number increases further to reach 1×10^5 cells per dish at D12, corresponding to a considerable hematopoietic production considering the relatively low number of cells seeded at culture onset. At the molecular level, qPCR analysis of *CD144*, *PU1* and *CD45* reveals an early loss of endothelial traits in floating cells, in keeping with the changes that occur during EHT *in vivo*, and a progressive increase in CD45 with time consistent with

Development (2016) 143, 1302-1312 doi:10.1242/dev.126714

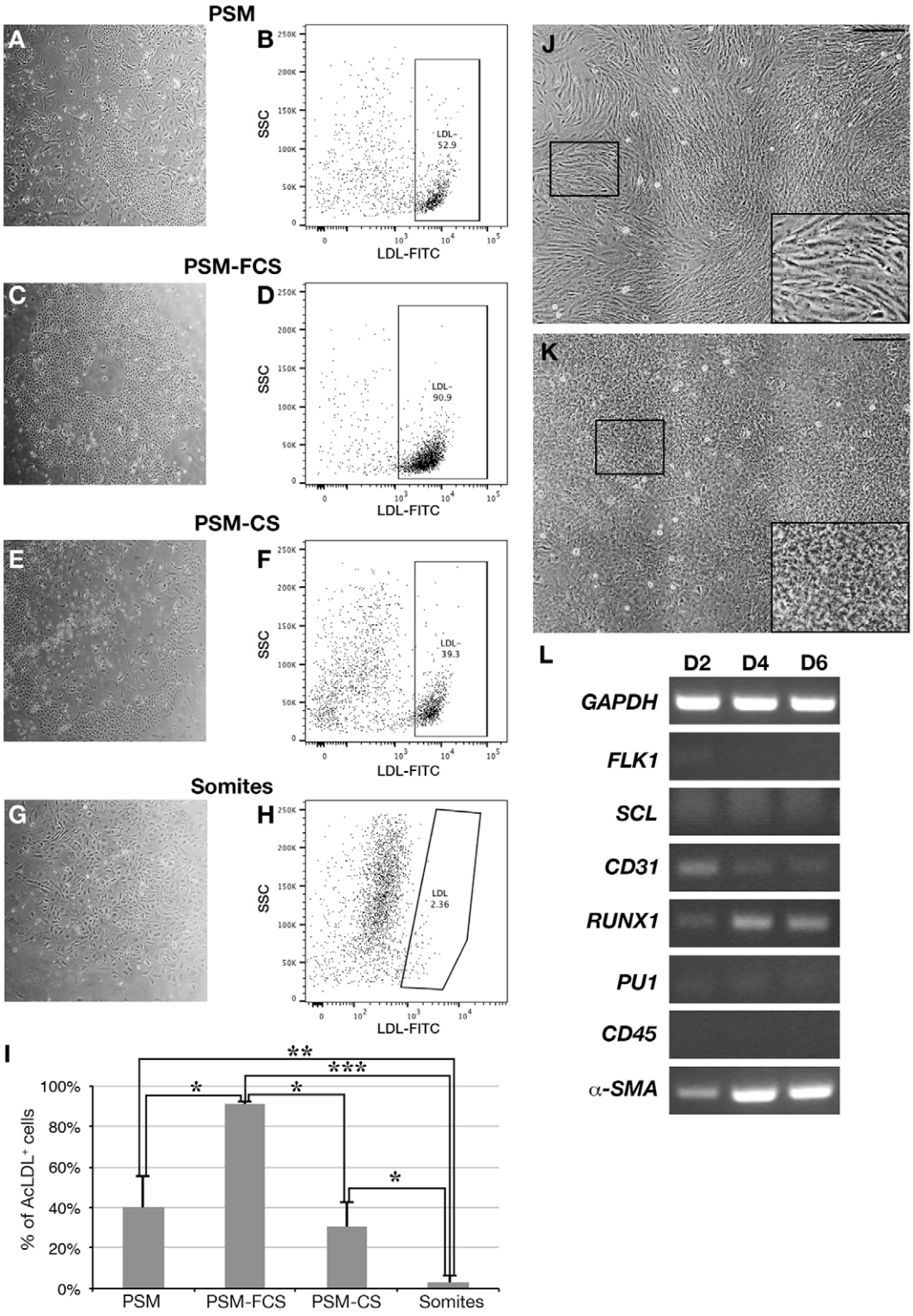

Fig. 5. EC differentiation depends on the tissue of origin and on medium composition. (A-I) Role of serum in EC differentiation. PSM in (A,B) standard conditions, (C,D) without FCS, (E,F) without CS, and (G,H) somites in standard conditions. Note the enhanced EC differentiation in the absence of FCS, with up to 90% of the cells positive for AcLDL uptake, and the poor differentiation that is shown by the somite cells. Dot plots are from individual representative experiments and are the result of 2000 events analyzed. (I) The percentage of AcLDL^{+} cells in the different experimental conditions. Data are mean±s.e.m. n=3. *P<0.01, **P<0.001, ***P<0.0001, Student's t-test. Analyses are the result of three independent experiments with three independent wells per experiment.
(J-L) Commitment to smooth muscle cells with TGFβ. (J,K) Phenotype of the culture at D4 (J) and D8 (K) following replacement of the initial set of growth factors by TGFβ. No endothelial-specific phenotype was visible during the culture period (12 days). No hematopoietic-like floating cell was visible. The rare floating cells are dead cells. Boxed regions are magnified in insets. Scale bars: 30 µm. (L) Semi-quantitative PCR analysis of the culture submitted to TGFβ. Cells were collected at D2, D4 and D6 and analyzed for the expression of several genes specific for endo-hematopoietic cells and for the alpha smooth muscle actin isoform (*αSMA*) that is specific for smooth muscle cells. Low to nil expression of endo-hematopoietic genes was found, whereas cells displayed increased expression of *αSMA*, indicative of smooth muscle cell commitment.

Development (2016) 143, 1302-1312 doi:10.1242/dev.126714

maturation of the recently produced HCs (Jaffredo et al., 2005a; Zape and Zovein, 2011). This sustained hematopoietic production is indeed due to the EHT that persists with time in culture, and also to hematopoietic cell multiplication. Future work will be needed to quantify the relative importance of these two events.

The hematopoietic cells that are produced differentiate into several hematopoietic lineages, as testified by the presence of at least three morphologically distinct types of hematopoietic cell – granulocytes, monocytes and erythroblasts – originating from three distinct types of progenitor. The lack of avian recombinant cytokines precludes a thorough clonogenic identification of the progenitor cells produced in culture. Further work will be necessary to examine whether lymphocytes, and eventually HSPCs, could also be produced. The differential expression of *PU1*, which is a direct target of RUNX1 (Huang et al., 2008), and *CD45* between D4 and D6 indicates that the newly formed HSPCs undergo progressive maturation in culture.

Owing to the limitations mentioned above and the short duration of the process, capturing hemogenic ECs undergoing EHT remains a challenge in culture. A large number of cells experiencing EHT are visible from D4. This unique situation would allow the isolation of hemogenic ECs undergoing EHT for analysis by various approaches. Investigation of the culture conditions has shown that it is possible to reinforce EC differentiation or to anticipate EHT by modulating the presence of FCS and VEGF. Our aim is to exploit this versatility to find a way to collect sufficient numbers of cells undergoing EHT for further cellular and molecular analyses.

In addition to ECs and hemogenic ECs, we demonstrate that it is possible to direct the culture towards the smooth muscle cell lineage by modulating the combination of growth factors. This opens the way to study, in greater depth, the molecular choices made by mesoderm cells during differentiation. This will also help to more accurately identify key factors involved in the EHT process from future high-throughput data. Given the versatility of the culture system, one could also envision its use to manipulate the PSM cells to produce striated muscle or tendon precursors, two cell types also derived following differentiation of the somite.

Taken together, our results provide a new and versatile system with which to study commitment to hemogenic ECs and the EHT. Future in-depth analysis of the molecular pathways involved in these processes will have important implications for the understanding of EHT and the search for key hematopoietic inducing signals and molecular pathways that are crucial in directing the production of HSPCs from the hemogenic endothelium.

MATERIALS AND METHODS

PSM isolation

We used quail (*Coturnix coturnix japonica*) embryo PSM, handled according to Fig. 1A. Eggs were incubated for 36-45 h at 37±1°C in a humidified atmosphere to reach 10-18 somite pairs. Microsurgery was performed as previously described (Pardanaud et al.,1996). The PSM was removed over a length corresponding to ten somites from both sides of the embryo. Five embryos (i.e. ten PSMs) were used per culture dish. Each PSM was cut into five or six equal pieces and rinsed in Opti-MEM plus GlutaMAX I containing 5% fetal calf serum (FCS), 100 units/ml penicillin/streptomycin and 1% chicken serum (CS) (all Gibco Life Technologies) before culture. Avian embryo care and procedures were in accordance with national and European laws.

Culture conditions

PSM was cultured in Opti-MEM with GlutaMAX I supplemented with 5% FCS, 1% chicken serum, 100 units/ml penicillin/streptomycin and the following growth factors (PromoCell/PromoKine unless stated otherwise): human VEGF (C64410; 2 ng/ml), human FGF (C60240; 4 ng/ml), human IGF (C60840; 3 ng/ml), human EGF (C60170; 10 ng/ml), hydrocortisone (Sigma, H6909; 200 ng/ml) and ascorbic acid (Sigma, A4544; 75 µg/ml). To promote smooth muscle cell differentiation, the growth factors were replaced by TGFβ (PromoCell/PromoKine, C63500; 25 ng/ml). PSM was cultured in Corning BioCoat 35 mm collagen I- or IV-coated dishes (Corning-Dutscher). Medium was changed every 2 days unless otherwise specified.

RNA extraction and qRT-PCR

RNA extractions were performed using the RNeasy Kit (Qiagen). Freshly isolated PSM (ten) were resuspended in the RNeasy buffer solution (RLT). For RNA extraction from cultured cells, the cells were first centrifuged (300 ***g*** for 10 min) to remove the medium and resuspended in RLT. Adherent cells were first trypsinized, washed in PBS containing 10% FCS, centrifuged and then resuspended in RLT. Quality and quantity of the extracted RNA was evaluated using Nanodrop. The primers used for semi-quantitative RT-PCR and for qPCR are listed in Table S1. PCR was performed on an Eppendorf Mastercycler Epgradient S. qPCR was performed using the LightCycler 480 (Roche) real-time system according to the manufacturer's instructions. Relative expression was calculated as $2^{[Ct(\text{gene of interest})-Ct(\text{gene of reference})]}$.

Immunostaining and DAPI staining of *in vitro* culture

We used acetylated low-density lipoprotein from human plasma coupled to Alexa Fluor 488 (AcLDL-A488; 1 mg/ml; Life Technologies, L23380, batches 1291485 and 1696210), the QH1 monoclonal antibody developed by Pardanaud et al. (1987) (obtained from the Developmental Studies Hybridoma Bank, created by the NICHD of the NIH and maintained at The University of Iowa, Department of Biology, Iowa City, IA 52242, USA) and antibody against RUNX1 (Abcam, ab92336, batches GR107772-3 and 107772-5) to determine the endothelial phenotype of PSM-derived cells. AcLDL-A488 (1/100 in PBS) was incubated together with QH1 antibody (1/20 in PBS) for 30 min at 37°C in the culture dish.

After three washes in PBS, goat anti-mouse IgG1 secondary antibody coupled to Alexa Fluor 555 (Molecular Probes; 1/100 in PBS), which recognizes QH1 antibody, was incubated for 30 min at 37°C. Cultures were then washed three times in PBS before imaging.

When RUNX1 was revealed, the cells were fixed following AcLDL uptake with 3.7% formaldehyde in PBS, rinsed three times with PBS containing 0.1% Triton X-100 for 10 min, incubated with the anti-RUNX1 antibody for 1 h at room temperature, followed by incubation with a goat anti-rabbit secondary antibody coupled to biotin (Southern Biotech, 4050-08) followed by three rinses in PBS (5 min each) and an incubation with Streptavidin-Cy3 (Invitrogen, 43-8315) diluted 1/500 in PBS.

To visualize nuclei, cultures were first fixed in 4% paraformaldehyde in PBS for 20 min, washed three times in PBS, and then incubated with DAPI in PBS containing 0.4% Triton X-100 for 20 min. After three washes in PBS, cultures were mounted with a coverslip before imaging on a Leica DM6000 B inverted microscope.

FACS analysis

Cells were stained with either AcLDL-A488 or with the QH1 monoclonal antibody. When adherent cells were used, cells were trypsinized and rinsed three times in PBS. When floating cells were used, cells were gently removed from the culture dish by pipetting. For AcLDL analysis, the cells were suspended in PBS containing 7-aminoactinomycin (7AAD) to exclude dead cells and analyzed with a MacsQuant analyzer 10 (Miltenyi Biotec). For QH1, cells were centrifuged, resuspended in PBS, incubated with the QH1 antibody (1/20) for 20 min at 4°C, washed in PBS and centrifuged. Cells were then incubated with goat anti-mouse IgG1-A488 (Molecular Probes; 1/100 in PBS) for 20 min at 4°C, washed in PBS and centrifuged. Finally, cells were resuspended in PBS containing 7AAD to exclude dead cells and analyzed on a FACSAria III (BD Biosciences) or on a MacsQuant analyzer 10. Analyses were performed with FlowJo 10. Statistics were performed with GraphPad Prism.

May–Grünwald Giemsa staining

Floating cells were gently removed from the culture dish by pipetting, washed, centrifuged and suspended in PBS before proceeding to cytospin (Cytocentrifuge, Shandon-Elliot). Glass slides with the spot of cells were

Development (2016) 143, 1302-1312 doi:10.1242/dev.126714

covered with May–Grünwald solution (Merck) for 3 min at room temperature. Five or six drops of PBS were added to the May–Grünwald solution directly on the slide, mixed gently, and incubated for another 3 min. Slides were then rinsed with PBS and covered with diluted Giemsa (1/10; Merck) for 20 min. Slides were finally washed with distilled water and air dried. Slides were mounted with a coverslip and a few drops of Entellan (Sigma). Images were taken on a Nikon Eclipse E800 microscope.

EHT tracking

Movies were recorded on a Leica DM6000 B inverted microscope at 37°C and 5% CO_2 with a 10× objective. Images were acquired every 10 min using a CoolSnap HQ2 camera (1392×1040 imaging pixels; Photometrics) over a mean period of 24 h using Leica MMAF software v1.6.0. Films were analyzed using ImageJ (NIH). The tracking was made in two steps because of the two cell morphologies. In the first step, and because before undergoing EHT there is little movement in the flat layer of ECs, the cell undergoing phenotypic changes is marked at the time or immediately after the time (user choice) of EHT. A circle is drawn to localize the cell based on its Cartesian coordinates. From this point, a second window is opened that will allow the user to trace the same cell back in time to before EHT (the number of frames back is also a user choice). The macro is available upon request. In the second step, the algorithm automatically finds the brightest points around the previous cell localization and selects the closest coordinates. Movies have been assembled and labeled using Final Cut Pro (Apple).

Acknowledgements

We thank Drs Charles Durand and Cecile Drevon for critical reading of the manuscript; Laurence Petit for efficient help in flow cytometry; and Sophie Gournet for excellent photographic and drawing assistance.

Competing interests

The authors declare no competing or financial interests.

Author contributions

L.Y., R.G. and T.J. designed experiments. L.Y., R.G., H.K., S.M. and M.S. performed experiments. J.-F.G. developed the cell-tracking program. L.Y., R.G., H.K. and T.J. analyzed data. L.Y. and T.J. wrote the paper.

Funding

This study was supported by grants from the Fondation pour la Recherche Médicale [DEQ20100318258] and Agence Nationale pour la Recherche/California Institute for Regenerative Medicine [ANR/CIRM 0001-02].

Supplementary information

Supplementary information available online at
http://dev.biologists.org/lookup/suppl/doi:10.1242/dev.126714/-/DC1

References

Asahara, T., Bauters, C., Zheng, L. P., Takeshita, S., Bunting, S., Ferrara, N., Symes, J. F. and Isner, J. M. (1995). Synergistic effect of vascular endothelial growth factor and basic fibroblast growth factor on angiogenesis in vivo. *Circulation* **92**, 365-371.

Bertrand, J. Y., Chi, N. C., Santoso, B., Teng, S., Stainier, D. Y. R. and Traver, D. (2010). Haematopoietic stem cells derive directly from aortic endothelium during development. *Nature* **464**, 108-111.

Boisset, J.-C., van Cappellen, W., Andrieu-Soler, C., Galjart, N., Dzierzak, E. and Robin, C. (2010). In vivo imaging of haematopoietic cells emerging from the mouse aortic endothelium. *Nature* **464**, 116-120.

Chen, M. J., Yokomizo, T., Zeigler, B. M., Dzierzak, E. and Speck, N. A. (2009). Runx1 is required for the endothelial to haematopoietic cell transition but not thereafter. *Nature* **457**, 887-891.

Choi, K., Kennedy, M., Kazarov, A., Papadimitriou, J. C. and Keller, G. (1998). A common precursor for hematopoietic and endothelial cells. *Development* **125**, 725-732.

Christ, B., Huang, R. and Scaal, M. (2007). Amniote somite derivatives. *Dev. Dyn.* **236**, 2382-2396.

de Bruijn, M. F. T. R., Ma, X., Robin, C., Ottersbach, K., Sanchez, M.-J. and Dzierzak, E. (2002). Hematopoietic stem cells localize to the endothelial cell layer in the midgestation mouse aorta. *Immunity* **16**, 673-683.

De Val, S. and Black, B. L. (2009). Transcriptional control of endothelial cell development. *Dev. Cell* **16**, 180-195.

Ditadi, A., Sturgeon, C. M., Tober, J., Awong, G., Kennedy, M., Yzaguirre, A. D., Azzola, L., Ng, E. S., Stanley, E. G., French, D. L. et al. (2015). Human definitive haemogenic endothelium and arterial vascular endothelium represent distinct lineages. *Nat. Cell Biol.* **17**, 580-591.

Dzierzak, E. and Speck, N. A. (2008). Of lineage and legacy: the development of mammalian hematopoietic stem cells. *Nat. Immunol.* **9**, 129-136.

Eilken, H. M., Nishikawa, S.-I. and Schroeder, T. (2009). Continuous single-cell imaging of blood generation from haemogenic endothelium. *Nature* **457**, 896-900.

Elefanty, A. G., Robb, L., Birner, R. and Begley, C. G. (1997). Hematopoietic-specific genes are not induced during in vitro differentiation of scl-null embryonic stem cells. *Blood* **90**, 1435-1447.

Guo, R., Sakamoto, H., Sugiura, S. and Ogawa, M. (2007). Endothelial cell motility is compatible with junctional integrity. *J. Cell. Physiol.* **211**, 327-335.

Hirashima, M., Ogawa, M., Nishikawa, S., Matsumura, K., Kawasaki, K., Shibuya, M. and Nishikawa, S.-I. (2003). A chemically defined culture of VEGFR2+ cells derived from embryonic stem cells reveals the role of VEGFR1 in tuning the threshold for VEGF in developing endothelial cells. *Blood* **101**, 2261-2267.

Huang, G., Zhang, P., Hirai, H., Elf, S., Yan, X., Chen, Z., Koschmieder, S., Okuno, Y., Dayaram, T., Growney, J. D. et al. (2008). PU.1 is a major downstream target of AML1 (RUNX1) in adult mouse hematopoiesis. *Nat. Genet.* **40**, 51-60.

Huber, T. L., Kouskoff, V., Fehling, H. J., Palis, J. and Keller, G. (2004). Haemangioblast commitment is initiated in the primitive streak of the mouse embryo. *Nature* **432**, 625-630.

Jaffredo, T., Gautier, R., Eichmann, A. and Dieterlen-Lièvre, F. (1998). Intraaortic hemopoietic cells are derived from endothelial cells during ontogeny. *Development* **125**, 4575-4583.

Jaffredo, T., Bollerot, K., Sugiyama, D., Gautier, R. and Drevon, C. (2005a). Tracing the hemangioblast during embryogenesis: developmental relationships between endothelial and hematopoietic cells. *Int. J. Dev. Biol.* **49**, 269-277.

Jaffredo, T., Nottingham, W., Liddiard, K., Bollerot, K., Pouget, C. and de Bruijn, M. (2005b). From hemangioblast to hematopoietic stem cell: an endothelial connection? *Exp. Hematol.* **33**, 1029-1040.

Kispert, A., Ortner, H., Cooke, J. and Herrmann, B. G. (1995). The chick Brachyury gene: developmental expression pattern and response to axial induction by localized activin. *Dev. Biol.* **168**, 406-415.

Kissa, K. and Herbomel, P. (2010). Blood stem cells emerge from aortic endothelium by a novel type of cell transition. *Nature* **464**, 112-115.

Lam, E. Y. N., Hall, C. J., Crosier, P. S., Crosier, K. E. and Flores, M. V. (2010). Live imaging of Runx1 expression in the dorsal aorta tracks the emergence of blood progenitors from endothelial cells. *Blood* **116**, 909-914.

Lamalice, L., Le Boeuf, F. and Huot, J. (2007). Endothelial cell migration during angiogenesis. *Circ. Res.* **100**, 782-794.

Lancrin, C., Sroczynska, P., Stephenson, C., Allen, T., Kouskoff, V. and Lacaud, G. (2009). The haemangioblast generates haematopoietic cells through a haemogenic endothelium stage. *Nature* **457**, 892-895.

Lancrin, C., Sroczynska, P., Serrano, A. G., Gandillet, A., Ferreras, C., Kouskoff, V. and Lacaud, G. (2010). Blood cell generation from the hemangioblast. *J. Mol. Med.* **88**, 167-172.

Medvinsky, A., Rybtsov, S. and Taoudi, S. (2011). Embryonic origin of the adult hematopoietic system: advances and questions. *Development* **138**, 1017-1031.

Newman, P. J., Berndt, M. C., Gorski, J., White, G. C., II, Lyman, S., Paddock, C. and Muller, W. A. (1990). PECAM-1 (CD31) cloning and relation to adhesion molecules of the immunoglobulin gene superfamily. *Science* **247**, 1219-1222.

North, T. E., de Bruijn, M. F. T. R., Stacy, T., Talebian, L., Lind, E., Robin, C., Binder, M., Dzierzak, E. and Speck, N. A. (2002). Runx1 expression marks long-term repopulating hematopoietic stem cells in the midgestation mouse embryo. *Immunity* **16**, 661-672.

Pardanaud, L. and Dieterlen-Lièvre, F. (1999). Manipulation of the angiopoietic/hemangiopoietic commitment in the avian embryo. *Development* **126**, 617-627.

Pardanaud, L., Altmann, C., Kitos, P., Dieterlen-Lièvre, F. and Buck, C. A. (1987). Vasculogenesis in the early quail blastodisc as studied with a monoclonal antibody recognizing endothelial cells. *Development* **100**, 339-349.

Pardanaud, L., Luton, D., Prigent, M., Bourcheix, L.-M., Catala, M. and Dieterlen-Lièvre, F. (1996). Two distinct endothelial lineages in ontogeny, one of them related to hemopoiesis. *Development* **122**, 1363-1371.

Pepper, M. S., Ferrara, N., Orci, L. and Montesano, R. (1992). Potent synergism between vascular endothelial growth factor and basic fibroblast growth factor in the induction of angiogenesis in vitro. *Biochem. Biophys. Res. Commun.* **189**, 824-831.

Pouget, C., Gautier, R., Teillet, M.-A. and Jaffredo, T. (2006). Somite-derived cells replace ventral aortic hemangioblasts and provide aortic smooth muscle cells of the trunk. *Development* **133**, 1013-1022.

Pourquie, O. (2003). Vertebrate somitogenesis: a novel paradigm for animal segmentation? *Int. J. Dev. Biol.* **47**, 597-603.

Richard, C., Drevon, C., Canto, P.-Y., Villain, G., Bollérot, K., Lempereur, A., Teillet, M.-A., Vincent, C., Rosselló Castillo, C., Torres, M. et al. (2013). Endothelio-mesenchymal interaction controls runx1 expression and modulates the notch pathway to initiate aortic hematopoiesis. *Dev. Cell* **24**, 600-611.

Development (2016) 143, 1302-1312 doi:10.1242/dev.126714

Robertson, S. M., Kennedy, M., Shannon, J. M. and Keller, G. (2000). A transitional stage in the commitment of mesoderm to hematopoiesis requiring the transcription factor SCL/tal-1. *Development* **127**, 2447-2459.

Seghezzi, G., Patel, S., Ren, C. J., Gualandris, A., Pintucci, G., Robbins, E. S., Shapiro, R. L., Galloway, A. C., Rifkin, D. B. and Mignatti, P. (1998). Fibroblast growth factor-2 (FGF-2) induces vascular endothelial growth factor (VEGF) expression in the endothelial cells of forming capillaries: an autocrine mechanism contributing to angiogenesis. *J. Cell Biol.* **141**, 1659-1673.

Swiers, G., Baumann, C., O'Rourke, J., Giannoulatou, E., Taylor, S., Joshi, A., Moignard, V., Pina, C., Bee, T., Kokkaliaris, K. D. et al. (2013). Early dynamic fate changes in haemogenic endothelium characterized at the single-cell level. *Nat. Commun.* **4**, 2924.

Tavian, M., Coulombel, L., Luton, D., San Clemente, H., Dieterlen-Lièvre, F. and Péault, B. (1996). Aorta-associated $CD34^+$ hematopoietic cells in the early human embryo. *Blood* **87**, 67-72.

Vogeli, K. M., Jin, S.-W., Martin, G. R. and Stainier, D. Y. R. (2006). A common progenitor for haematopoietic and endothelial lineages in the zebrafish gastrula. *Nature* **443**, 337-339.

Wagner, D. D., Olmsted, J. B. and Marder, V. J. (1982). Immunolocalization of von Willebrand protein in Weibel-Palade bodies of human endothelial cells. *J. Cell Biol.* **95**, 355-360.

Whelan, M. C. and Senger, D. R. (2003). Collagen I initiates endothelial cell morphogenesis by inducing actin polymerization through suppression of cyclic AMP and protein kinase A. *J. Biol. Chem.* **278**, 327-334.

Wilkinson, D. G., Bhatt, S. and Herrmann, B. G. (1990). Expression pattern of the mouse T gene and its role in mesoderm formation. *Nature* **343**, 657-659.

Wood, H. B., May, G., Healy, L., Enver, T. and Morriss-Kay, G. M. (1997). CD34 expression patterns during early mouse development are related to modes of blood vessel formation and reveal additional sites of hematopoiesis. *Blood* **90**, 2300-2311.

Yokomizo, T. and Dzierzak, E. (2010). Three-dimensional cartography of hematopoietic clusters in the vasculature of whole mouse embryos. *Development* **137**, 3651-3661.

Yvernogeau, L., Auda-Boucher, G. and Fontaine-Perus, J. (2012). Limb bud colonization by somite-derived angioblasts is a crucial step for myoblast emigration. *Development* **139**, 277-287.

Zape, J. P. and Zovein, A. C. (2011). Hemogenic endothelium: origins, regulation, and implications for vascular biology. *Semin. Cell Dev. Biol.* **22**, 1036-1047.

Zovein, A. C., Hofmann, J. J., Lynch, M., French, W. J., Turlo, K. A., Yang, Y., Becker, M. S., Zanetta, L., Dejana, E., Gasson, J. C. et al. (2008). Fate tracing reveals the endothelial origin of hematopoietic stem cells. *Cell Stem Cell* **3**, 625-636.

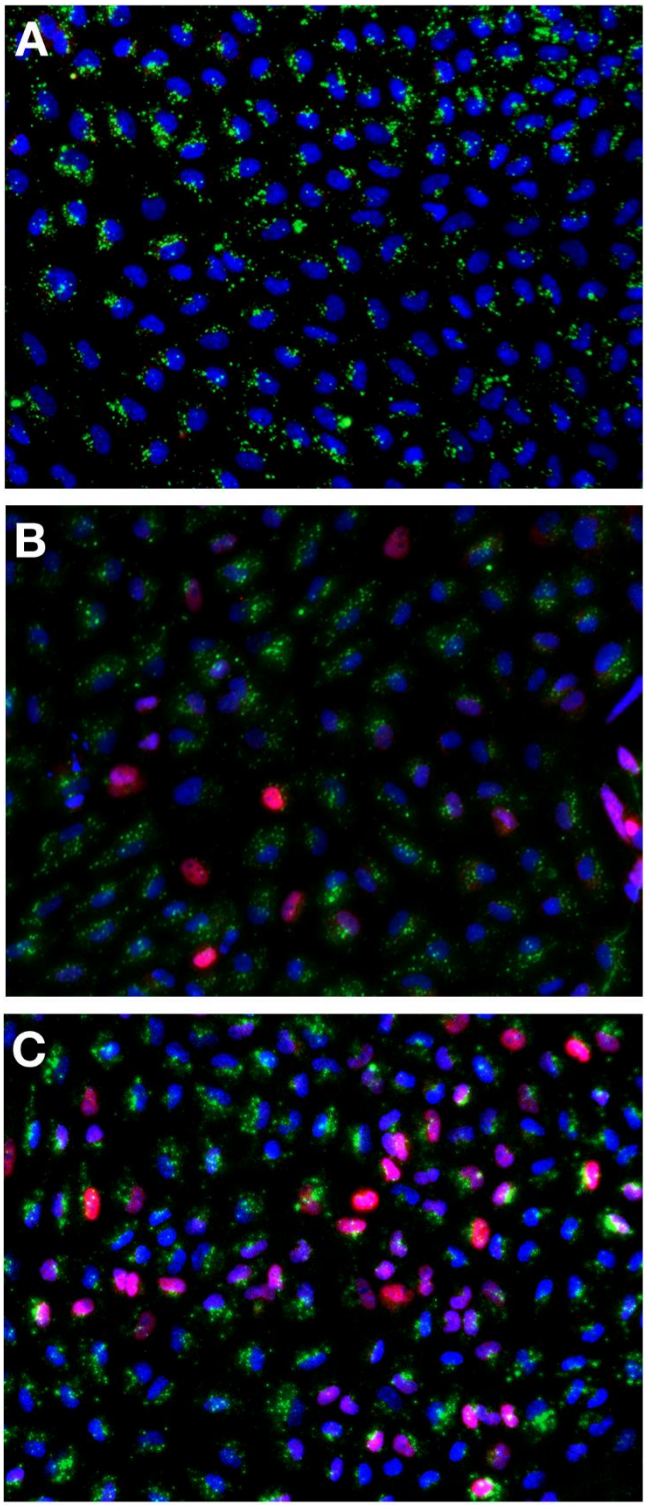

Fig. S1. Increase of RUNX1 staining in EC culture. Triple staining showing the use of human AcLDL uptake to reveal the ECs in green, the RUNX1 transcription factor expression as revealed by immunofluorescence in pink and the DAPI stained nuclei in blue at day 1 (A), 2 (B) and 3 (C) of culture. Note the growing number of RUNX1 positive nuclei with time.

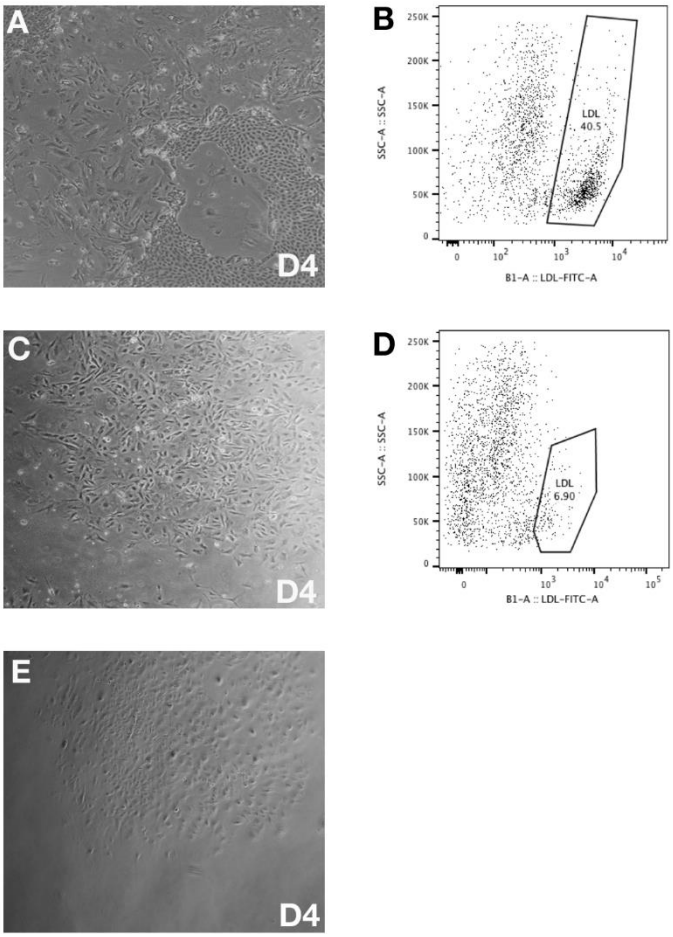

Fig. S2. Comparison between PSM, somites and lateral plate mesoderm isolated from embryos at the same somitic stage for their capacities to give rise to ECs. Dot plots are from one representative experiment. FACS analysis could not be performed for the lateral plate due to the low number of cells obtained. The dot plots are the result of 2000 events analyzed.

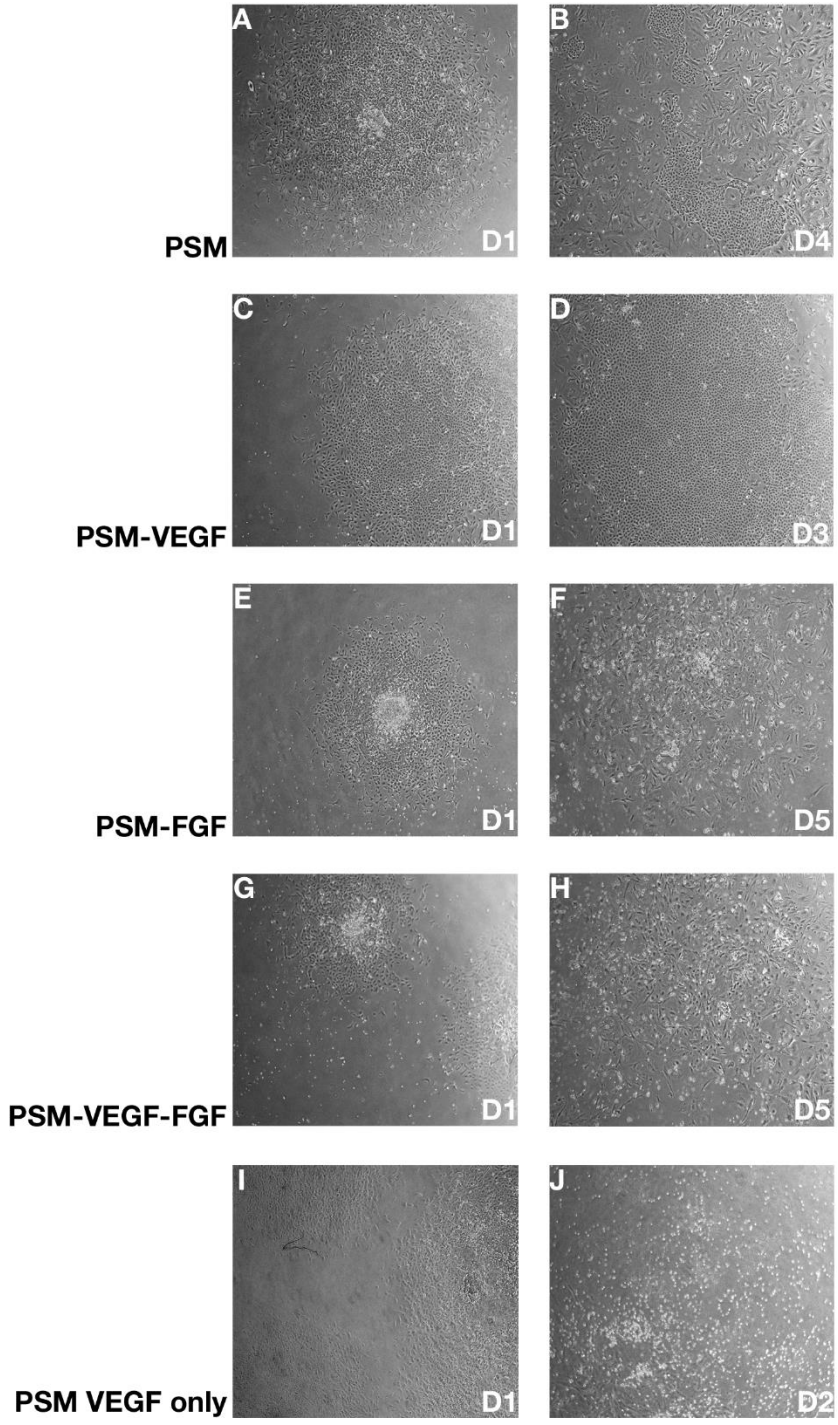

Fig. S3. PSM cultures in different growth factor conditions. In the absence of VEGF, PSM cells readily differentiate into flat, EC-like cells that are reminiscent of the cells obtained when PSM cells are placed in the absence of FCS (Figure 5C,D). When VEGF alone was added, an accelerated EC differentiation was observed quickly followed by a round, hematopoietic cell production. Cultures have been run from day (D) one to either D2 to 5 depending on the development of the culture.

Movie 1. Isolation of the PSM.

Movie 2. Spreading of a piece of PSM onto a collagen I-coated substrate during the first day of culture. Culture was followed over a period of 24 hours, at 37°C under 5% CO_2. The culture was imaged every ten minutes.

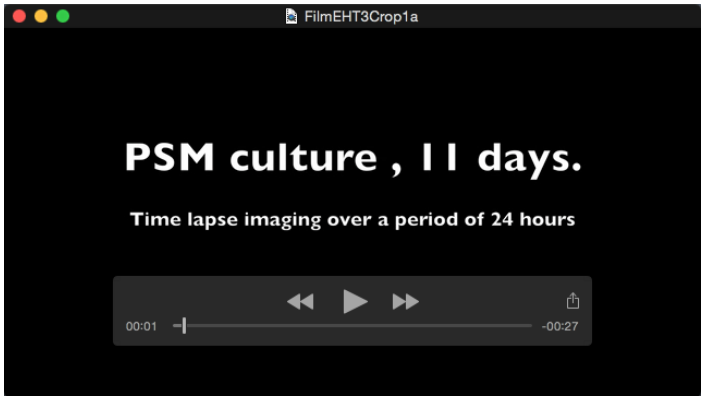

Movie 3. Multiplication of the non-adherent cell fraction followed over a period of 24 hours.

Movie 4. EHT tracking during the fourth day of culture over a period of 15h10. Cells undergoing EHT are numbered, circled in yellow and followed thereafter. Cell movement characteristics of EHT are clearly visible. Sequences displaying EHT have been decelerated to show specific individual cell movements.

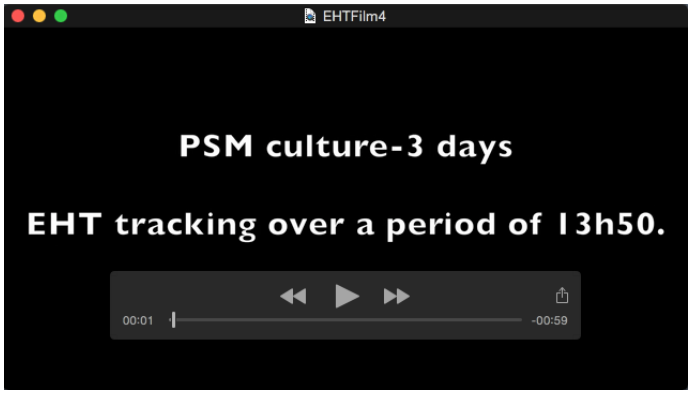

Movie 5. EHT tracking during the fourth day of culture over a period of 13h50.

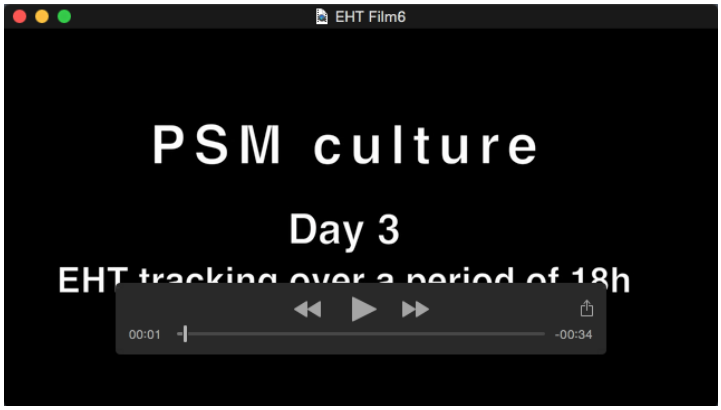

Movie 6. EHT tracking during the fourth day of culture over a period of 18h.

Table S1. Primers

Primers for semi-quantitative RT-PCR:

Gene	Orientation	Sequence	Localisation	Product size
Brachyury	Foward	TCCTCACTCTCAGTTTGGAGCACC	845	289
	Reverse	ACTCACGGACCATAAGTTCGGG	1133	
FLK1	Foward	AGGCTAAACATAGGCTGGGC	4602	383
	Reverse	AGAAGGCAGAGTGGCTTTCG	4984	
SCL	Foward	GAATGAAACATAGGGCTGTGG	1467	201
	Reverse	AGAAGGGAAAGGAAAGGGG	1667	
CD31	Foward	CACTTTTCTCTGCTCTGTGGAAG	1506	289
	Reverse	AATCATCACTCCTGCGATAGG	1794	
CD144	Foward	ATGTGTCCGTGCTCAACTCC	2088	294
	Reverse	GTCCCCAGTCATTTAGGAAGTC	2381	
CD34	Foward	ATCTGGTGGTGTCAGCAAGC	719	533
	Reverse	AGCCTTTCTTACAGCATCGG	1251	
vWF	Foward	GGTGTCATCCAATCCATCCACTG	4801	350
	Reverse	CAGCACTTTCAATAAATGCCCG	5129	
RUNX1	Foward	CCGATGGGACGCTGGTCAC	735	374
	Reverse	GTGGGTTGGGTGTGGGGG	1109	
PU1	Foward	TTACAGAACTGCAGAGCGTACAGC	201	423
	Reverse	CTTGCGATTGCCTTTCTGTATGCC	624	
CD45	Foward	GACCCTCTTGGAAAGTGCAGAAAC	3438	321
	Reverse	CCCCTTATTGGTATCTGCAGCCTT	3759	
c-KIT	Foward	CCCTTGCAGAGACCCACATTCAAA	2679	201
	Reverse	CCACTCAAACATCTTCGCGTACCA	2880	
GAPDH	Foward	CAGGTGCTGAGTATGTTGTGGAGTC	78	274
	Reverse	CTTCTGTGTGGCTGTGATGGC	351	

Primers used for QPCR:

Gene	Orientation	Sequence	Localisation	Product size
FLK1 L2093	Foward	GCGTTCCTCCTCCAAACATC	2093	127
FLK1 R2220	Reverse	CAGCCCTCCATCTTCTTTCC	2220	
CD144 gal L291	Foward	ACCACATCACGTTGGCAAGCTCAC	291	116
CD144 gal R407	Reverse	TGTCGCCATCGTACCCTTGCACT	407	
CD45 gal L173	Foward	TGACCTCTGCCAGCTCTCTCTCCT	173	118
CD45 gal R291	Reverse	GGCTGTGGGAGAGGCACCAGT	291	
PU1 gal L258	Foward	CCCCTCATTCCCCCTCCCTCTGA	258	149
PU1 gal R407	Reverse	CTCACTGTGCACGTGGTGTGGATG	407	
QS17 Ga F 264	Foward	ACTGCCAAAGTGAGAGTGACAAGGC	264	149
QS17 Ga R 413	Reverse	GCTCCTCCGCTCAGGCAAAGC	413	
CKIT gal L2768	Foward	AACTTTTCCACTCCGCCTTC	2768	131
CKIT gal R2899	Reverse	TCTTCCAGATGCCACTCAAAC	2899	
MEOX1 Ga F631	Foward	AAAGGAGCACTCAGAAAGCCAGCC	631	115
MEOX1 GA R 746	Reverse	CGAATTCTGCCTCCAGCTCCCTCA	746	
QGATA2 Ga F 105	Foward	ACCAGCGCAGCTCCTACCTCC	105	142
QGATA2 Ga R 247	Reverse	GACTCCCGGTCAGGCGGGTA	247	
QRUNX1 Ga F 99	Foward	CACACAAGAGCGGGTCCGGG	99	107
QRUNX1 Ga R206	Reverse	CGGATCGGTTGTGGTTGATGATGCT	206	
BRA Gal L625	Foward	TCCCCGAGACCCAGTTCATCGC	625	149
BRA Gal R774	Reverse	GGTTGTCTCCCGCTTCCTCCATCA	774	